JOURNAL OF SOLID STATE CHEMISTRY 85, 235–250 (1990)

Chemically Twinned Phases in the Ag_2S–PbS–Bi_2S_3 System. Part I. Electron Microscope Study

A. SKOWRON* AND R. J. D. TILLEY

Division of Materials, School of Engineering, University of Wales College of Cardiff, Cardiff CF2 1XH, United Kingdom

Received August 3, 1988; in revised form November 27, 1989

Phases in the PbS-rich region of the Ag_2S–PbS–Bi_2S_3 system have been studied by high resolution transmission electron microscopy. In samples quenched from the melt or melted and annealed at 773 or 973 K a number of new chemically twinned phases have been found. Their structures contain *galena*-like slabs four-, five-, seven-, and eight-octahedra wide, joined along twin planes. Ordered phases predominate in the PbS-rich region of the phase diagram, while both ordered and disordered intergrowths occur in the PbS-poor region. The role of Ag in stabilizing slabs of *galena*-like material five- and eight-octahedra wide and its function in the formation of these twinned phases is discussed.

I. Introduction

In recent years there has been considerable interest in nonstoichiometric compounds which respond to changes in anion to cation ratio by the incorporation of planar faults rather than point defects (*1*). One such group is that in which twin planes are used to accommodate the changes in stoichiometry, the phenomenon being referred to as chemical twinning or unit cell twinning (*2*).

An example of this behavior is found in the PbS–Bi_2S_3 system. If PbS (*galena*) is reacted with Bi_2S_3 (*bismuthite*), two compounds form in the PbS-rich region, heyrovskyite, $Pb_{24}Bi_aS_{36}$, and lillianite, $Pb_{12}Bi_2S_{24}$. The structures of these two phases can be regarded as composed of narrower or wider twinned slabs of the parent *galena* structure as shown in Fig. 1 (*3–5*). The relationship between these structures suggests that a number of other phases could form, one being related to another simply by varying the widths of the *galena*-like slabs, to generate a homologous series of compounds. Recent investigations (*6–8*) have indicated that such a series does not seem to form in the PbS–Bi_2S_3 system. However, if Ag_2S is added to the system as an extra component, a number of other twinned phases, vikingite, eskimoite, ourayite, and treasurite, have been found to form (*9–12*).

The studies in which these results were reported, in common with most other previous work on the Ag_2S–PbS–Bi_2S_3 system, have been made using X-ray diffraction. This technique is limited when investigating a system such as that of interest here because the twin planes are not always well

* Present address: Institute for Materials Research, McMaster University, 1280 Main Street West, Hamilton, Ontario L8S 4M1, Canada.

0022-4596/90 $3.00

ordered, and the long unit cells of the phases are difficult to characterize with precision. Electron microscopy, on the other hand, has been found to be an ideal tool for such investigations, as disordered materials can be imaged and the nature of the disorder verified. It therefore seemed of interest to examine the system using this technique. The present paper presents the results of these electron microscopic studies. A number of new ordered twinned phases were found as well as an extensive disordered region where intergrowth between twinned structures occurred.

Geometry of the Lillianite Homologs

The phases of interest here are composed of slabs of *galena*-like structure in a twinned relationship one to another united along (311) planes; the indices referring to the cubic *galena* unit cell. In terms of the unit cells of the phases so created, the twin planes are chosen to be parallel to (010). The width of the *galena*-like slabs in a direction perpendicular to (010) varies and is characteristic of the phase in question.

In order to describe the structures of these materials a notation based on the width of the *galena*-like slabs has been proposed (*10*). This particular series is designated by the leter L to signify that all materials are homologs of the phase lillianite which, at present, is one end member of the series. In order to classify the structure of a given homolog one specifies the widths of the *galena*-like slabs on both sides of each (311) plane in terms of the numbers of octahedra running diagonally across the layers in the direction indicated by an arrow in Fig. 1. In this way a phase can be unequivocally characterized independently of its chemical formula. Thus lillianite has the symbol $L4,4$ as it is made up of two slabs, each of which is four octahedra wide, joined along (311) planes. In the same way

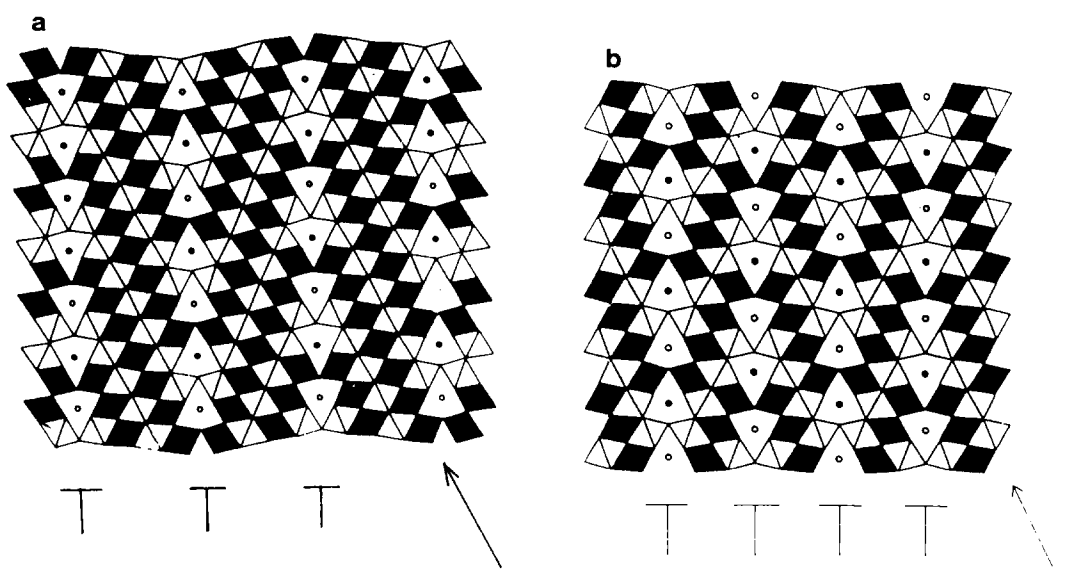

Fig. 1. The structures of (a) heyrovskyite and (b) lillianite projected onto (001). The structures are shown as packings of metal-sulphur octahedra; those at a lower level are light and those at a higher level are dark. Both structures can be regarded as made up of twinned slabs of PbS structure. The twin planes are marked T and the separation between them can be expressed in terms of the number of octahedra, N, counted in the direction of the arrows. For heyrovskyite, $N = 7$ and for lillianite, $N = 4$.

heyrovskyite is represented as *L*7,7 because it is made up of slabs seven octahedra wide. Generally. LN_1,N_2 is the symbol for a lillianite homolog in which the slabs of *galena*-like material have widths of N_1 and N_2 octahedra.

The most convenient and usual way of ascribing lattice parameters to a lillianite-related phase is to take the *a*-axis along the twin plane and the *c*-axis as perpendicular to the *a*-axis, e.g., parallel to [110] of PbS; this is approximately 0.4 nm for all the homologs. The *b*-axis is taken across the *galena*-like slabs in a direction as near as possible normal to the twin planes. This axis is the longest axis of each phase. The unit cell is orthorhombic for the phases where N_1 is equal to N_2. If N_1 differs from N_2 the symmetry becomes monoclinic.

There are a number of ways of establishing the values of N_1 and N_2 using only the geometrical characteristics of the electron diffraction patterns. Makovicky and Karup-Møller (*10*) used the angle between the reciprocal axes a^* and b^* to determine the number of octahedra across the layers. Only (001) zone-oriented diffraction patterns can be used for this purpose, but two pieces of information are immediately available from such patterns. First, measurements give approximate values of the axes *a* and *b* and a fairly precise value of the angle between them. Second from the intensity distribution of the reflections in the central (b^*) row of the diffraction pattern the value of $N_1 + N_2$ can be deduced. Further analysis of the geometry of the structures can lead to probable values of N_1 and N_2.

An alternative method of interpretation of electron diffraction patterns is described by VanDyck, Colaïtis, and Amelinckx (*13*). This does not require (001) zone-oriented diffraction patterns but the numbers N_1 and N_2 cannot be defined uniquely from one diffraction pattern. Instead a number of arbitrarily oriented diffraction patterns should be examined to determine the structure completely.

Experimental

All the samples studied in this investigation were prepared from elemental lead, bismuth, silver, and sulfur of "Specpure" grade supplied by Johnson Matthey Ltd. The quoted total metallic impurity content of each chemical did not exceed 10 ppm. The lead, which was in the form of 7-mm-diameter rods, was reduced to small pieces by paring with a fresh scalpel after initial removal of the outer surface of the rod. The bismuth was supplied in the form of lumps which were broken into fragments by the use of a percussion mortar. The sulfur and silver came as powders and were used without further treatment.

Thirty-six 1-gram samples were synthesized by the fursion of the elemental components in a variety of proportions in sealed and evacuated silica tubes. Full details of the compositions prepared and the X-ray phase analysis of the products is given elsewhere (*17*). The compositions analyzed in this study are shown in Fig. 2. All the samples were melted at approximately 1370 K and then cooled in one of three ways: (i) brine quenched from the melt, (ii) slow cooled to 773 K and then annealed at that temperature for 3 weeks before brine quenching, and (iii) slow cooled to 973 K and then annealed at that temperature for 7 days before brine quenching.

Electron microscope examination of samples made use of a Jeol 200CX electron microscope operationed at 200 kV. Electron microscope samples were prepared by crushing crystals in an agate mortar under *n*-butanol and allowing a drop or resultant suspension to dry on a copper grid previously coated with a holey carbon film. Thin regions of crystal were aligned using a top entry goniometer stage, to give reciprocal

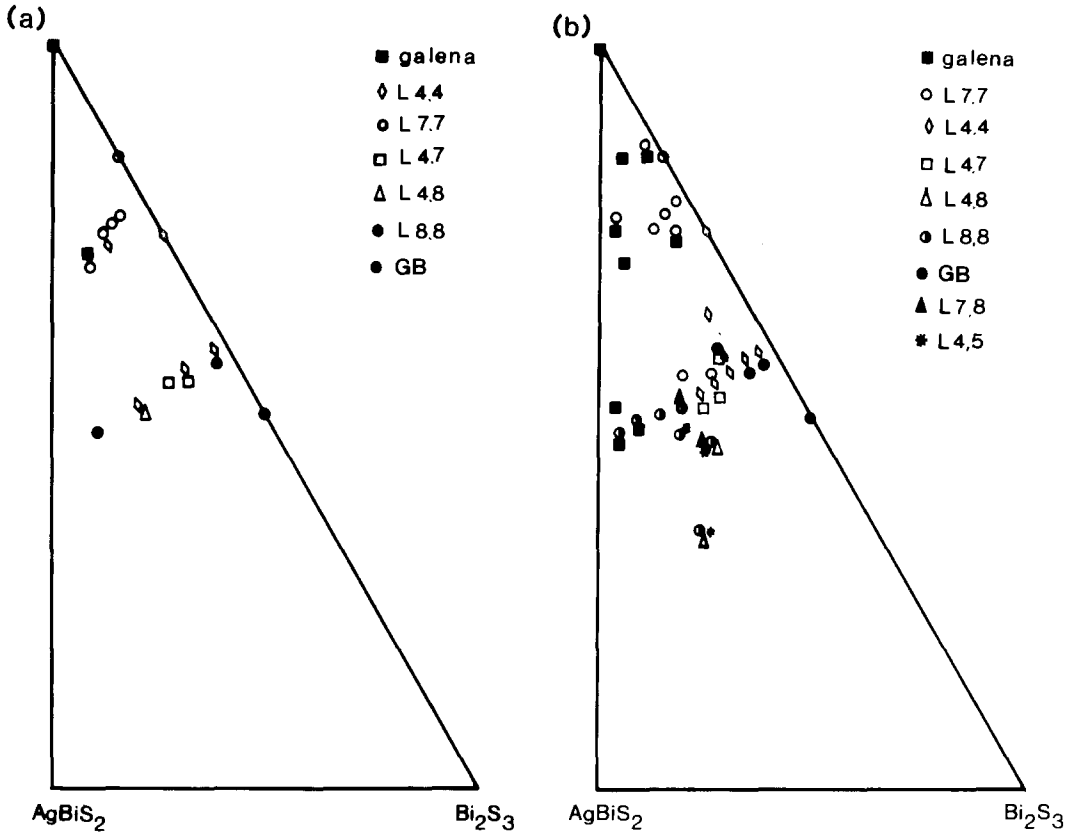

Fig. 2. Diagrammatic representations of the results of the electron microscope phase analysis: (a) samples annealed at 773 K, (b) samples annealed at 993 K. GB stands for galenobismuthite. (c) Tentative existence diagram of the Ag_2S–PbS–Bi_2S_3 system. The areas in which phases occur are approximated from (a) and (b). The exact compositions of the samples prepared are marked with dots and the line joining points in the lower part of the diagram indicates the region where the phases *L*7,7, *L*4,7, *L*4,4 intergrow.

lattice sections close to (001) zone axis projections.

Electron microscope phase analysis was carried out by measurement of (001) zone axis electron diffraction patterns as described above, and by direct measurement on electron micrographs taken under high resolution imaging conditions (*14*) or diffraction contrast conditions (*15*). When confirmation of image interpretation was necessary, images and electron diffraction patterns were computed using the EMS package of programs written by P. A. Stadelmann (*16*).

Results

In Fig. 2, we summarize the phases occurring at 773 and 973 K as determined by electron microscope phase analysis. A more complete phase analysis will be found in (*17*).

In the PbS-rich part of the system the phase analysis revealed the presence of two types of material, *galena* (PbS) and the twinned phases. Crystal fragments mostly consisted of only one phase. Intergrowth of galena and a twinned phase was not observed and intergrowth of two twinned

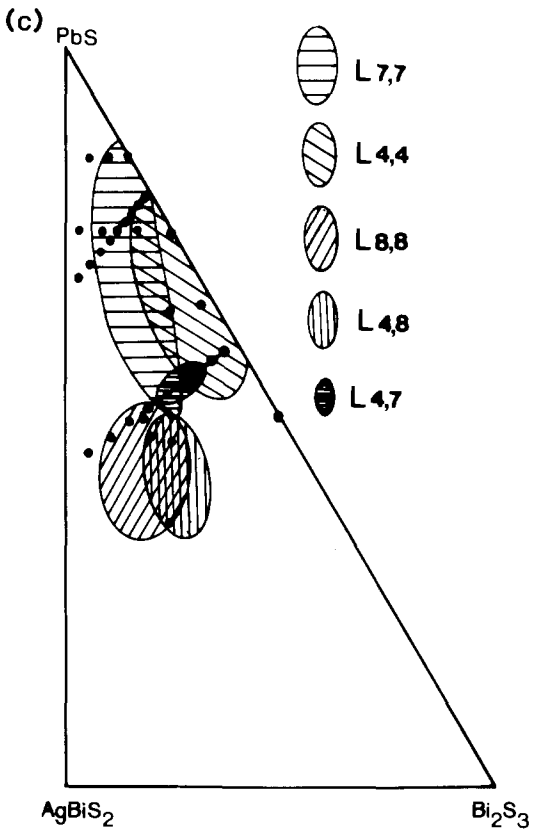

FIG. 2—*Continued*

phases was only very occasionally observed. The large number of PbS crystal flakes that were examined mostly revealed contrast characteristic of stoichiometric materials, albeit with occasional contrast typical of dislocations. Isolated twin planes similar to those shown in Fig. 3 were only rarely found. In the phase region furthest from PbS the situation was different, with considerable intergrowth between twinned phases occurring.

Ordered Phases

In the samples annealed at 773 K a number of previously reported ordered phases, *L*4,4, (lillianite), *L*4,7, (vikingite), *L*4,8 (treasurite), and *L*7,7, (heyrovskyite), were found. As an example, in Fig. 4 we show an electron diffraction pattern and image of the known phase *L*4,7. The crystal is slightly tilted with respect to the electron beam, and the alternating bands of *galena*-like material appear light and dark due to some degree of diffraction contrast. The diagonal lines on the bands are the (110) planes of the galena, as was confirmed by image simulations, some of which are shown in Fig. 4c. Measurement of the spacing between the twin planes was obtained with respect to the known (110) interplanar spacing of PbS, which confirmed the *L*4,7 structure. The interpretation of the electron diffraction pattern, shown in Fig. 4b, following the methods outlined above, agrees with this result. In this figure the reflection marked 0,15,0 corresponds to the 311 reflection of the PbS subcell. The electron diffraction pattern of another of these known phases, *L*4,8 (treasurite), is shown in Fig. 6b.

In addition to these known structures, a number of new phases, *L*4,5, *L*7,8 and *L*8,8, were positively identified. Figure 5 shows a micrograph of the phase *L*8,8. The contrast is principally due to diffraction contrast, but the resolution of the *galena* (110) planes in parts of the image allows the twin plane spacing to be accurately determined. The interpretation of the image was confirmed by the accompanying diffraction pattern. Similarly, the electron diffraction patterns shown in Figs. 6a and 6c confirm the presence of the structures, *L*4,5 and *L*7,8. In addition to these phases, one or two crystal fragments were found which are believed to be from the structures *L*5,7 and *L*5,8. Further work is needed before these can be confirmed.

Many of the samples annealed at 973 K were inhomogeneous and small needle-like crystals had often separated from the bulk. These were found to be *L*4,4, (lillianite). In the bulk material it was noted that two phases, *L*4,7, (vikingite) and *L*4,4, (lillianite) seemed to occur over wider areas in the composition diagram than at 773 K.

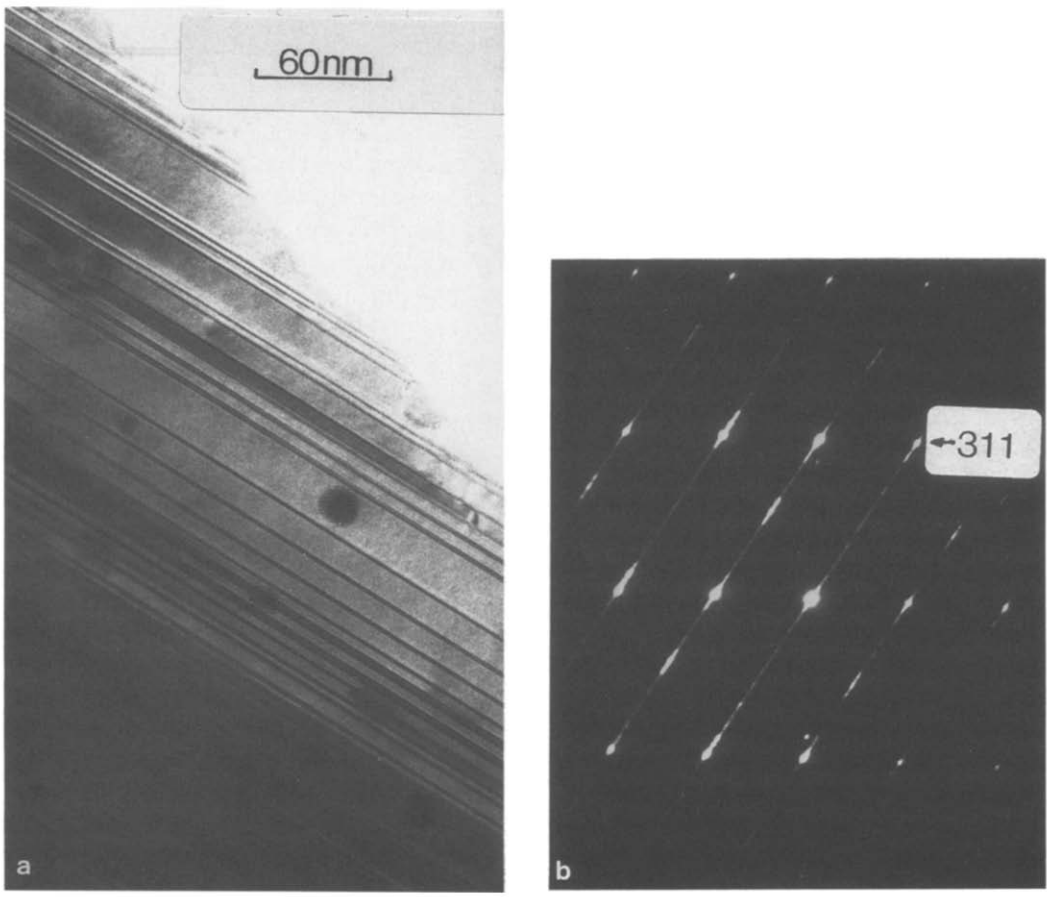

Fig. 3. (a) Electron micrograph showing isolated (311) twin planes, imaged as dark straight lines, in PbS. (b) The corresponding electron diffraction pattern, close to the (001) zone axis orientation, with the position of the PbS 311 reflection marked.

No ordered phases other than those listed above were found in the material which had been quenched from the melt.

Disordered Phases

Although the twinned phases did not seem to intergrow easily for PbS-rich compositions, a region with a great deal of disorder, marked with a line on Fig. 2c, was found for PbS-poorer material for all preparation conditions. The four twinned phases that were found in this region, $L8,8$, $L7,7$, $L4,7$, and $L4,4$, all had a strong tendency to intergrow. Various degrees of disorder were present in the intergrown material. Figure 7a shows an intergrowth between *galena*-like slabs seven and eight octahedra in width. This interpretation was confirmed by comparing the twin plane spacings with those of the *galena*-like (110) planes which are clearly resolved at the crystal edges and with computed images expected from the $L7,7$ and $L8,8$ structures. The reflections on the corresponding diffraction pattern, Fig. 7b, can be separated into two sets of superimposed, slightly differently spaced reflections that correspond to $L7,7$ and $L8,8$, indicating that in some regions quite

extensive volumes of these structures occur. Figure 8a shows an example of an irregular intergrowth. As well as much wider *galena*-like regions, *galena*-like slabs with widths of four, seven, and eight octahedra can be distinguished which appear to indicate a tendency to a mixture of *L*4,7, *L*4,8, and *L*7,8 phases. The corresponding diffraction pattern, Fig. 8b, reveals considerable streaking between the reflections in the central row.

Two examples of intergrown material found in the area of compositions where *L*4,4 and *L*4,7 coexisted are shown in Figs. 9 and 10. The spacing of the lattice fringes on the micrograph Fig. 9a indicates that the twin slabs have widths of four and seven octahedra. The diffraction pattern, shown in Fig. 9b, however, is rather similar to that from lillianite, suggesting that adjacent areas of the crystal fragment are predominantly composed of the *L*4,4 phase. The tendency of these intergrowths to form sequences of *L*7,4, *L*7,4,4, *L*7,4,4,4, and *L*7,4,4,4,4 type is revealed by Fig. 10a. Here the wider white strips correspond to slabs seven octahedra in width and the narrower strips to slabs four octahedra in width. The diffraction pattern shown in Fig. 10b, although not very sharp, indicates a tendency to an average repeat distance of approximately 6.6 nm. This corresponds to the observed *L*7,4,4 sequence.

In the PbS-poorest compositions studied, where *L*4,8 and *L*8,8 twined phases coexisted, the tendency of the material to intergrow seemed to decrease, and usually the crystal fragments contained only one structure. However, a few crystal fragments which revealed disordered intergrowths of *L*4,4 and *L*4,8 were found. Further study is desirable in this region.

Discussion

The results presented above have shown that besides the phases already reported, viz. *L*4,4, *L*4,7, *L*4,8, and *L*7,7, a number of new ordered phases, *L*4,5, *L*7,8, *L*8,8, and two tentative phases, *L*5,7 and *L*5,8, occur in the galena-rich region of the Ag_2S–PbS–Bi_2S_3 system. In addition, the structure of some intergrowths showed a tendency toward rather complex repeat units which indicates that more new phases may form under different preparation conditions.

In the PbS–Bi_2S_3 system it seems that only the ordered orthorhombic phases *L*4,4 and *L*7,7 are stable. The present study shows clearly that the addition of Ag_2S to the system stabilizes *galena*-like slabs of widths five and eight octahedra. However, it is noticeable that neither of the structures *L*5,5 nor *L*6,6 were found in the present series of preparations. Moreover, of the phases containing slabs five octahedra in width, only the *L*4,5 phase was well documented. The others observed, *L*5,7 and *L*5,8, were recorded only in a very few fragments. The other important difference the addition of Ag has made, compared to the ternary system, is in stabilizing monoclinic structures of the type LN_1,N_2. Despite a considerable amount of effort, phases of the sort *L*4,7 have not been detected in the ternary system, yet in the Ag_2S–PbS–Bi_2S_3 system the *L*4,7 structure was readily found.

Comparison of our results with the reports of Makovicky and Karup-Møller on naturally occurring twinned sulfosalts (*9–12*) shows that two of the phases reported by these authors, *L*5,9 (eskimoite) and *L*11,11 (ourayite), were not found in this study. We specifically searched for these phases in samples with overall compositions corresponding to their idealized formulae, but without success.

A possible explanation for the absence of the phases *L*5,9 and *L*11,11 could lie in thermal stability. It was found that *L*4,4, (lillianite), the phase with the narrowest slabs, seems to have enhanced stability at 973 compared to 773 K, as it occurred over

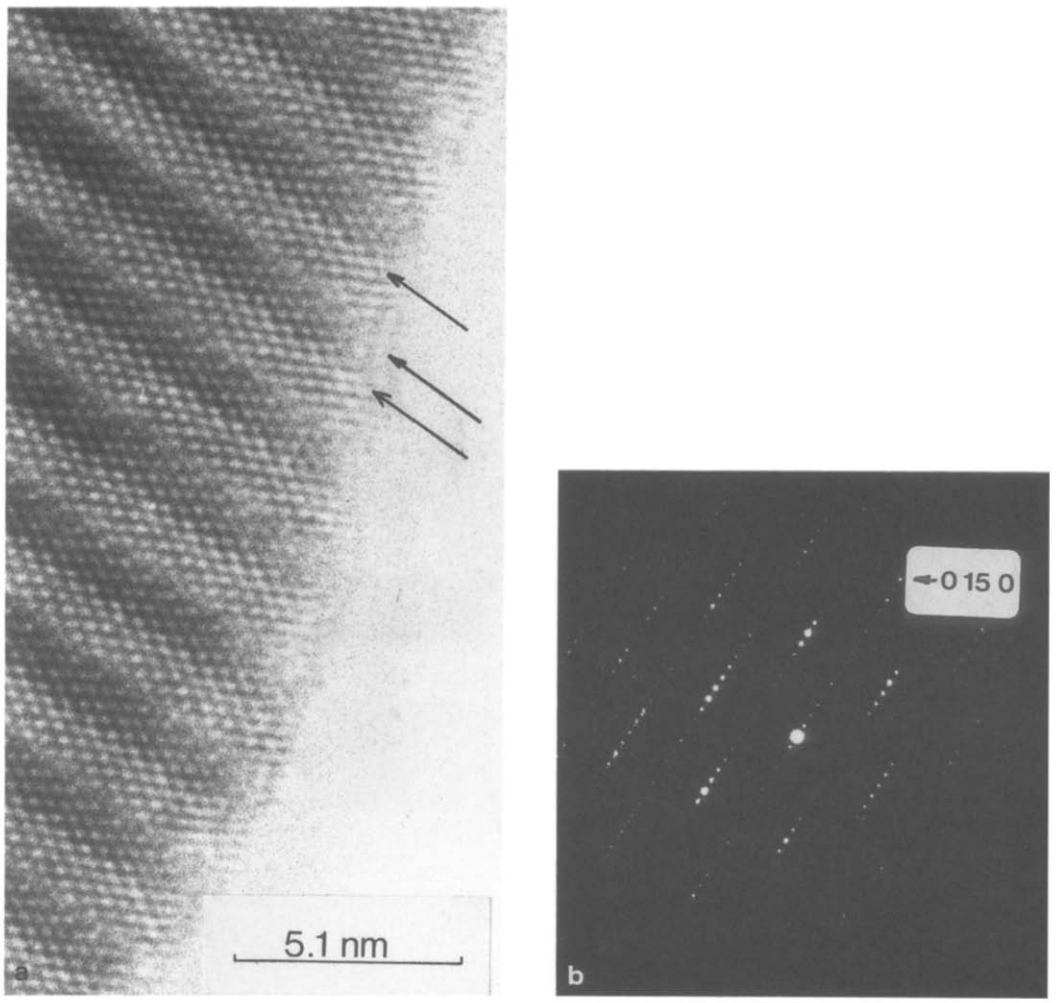

Fig. 4. (a) Electron micrograph, (b) electron diffraction pattern, and (c) calculated images of *L*4,7 close to the (001) projection. The *galena*-like slabs are imaged with alternate light and dark contrast typical of twinned structures. Some twin planes are arrowed. The diagonal lines are the (110) planes of the *galena*-like matrix. The 0,15,0 reflection on (b) corresponds to the 311 reflection of the PbS subcell. The images (c) were calculated at defocus values of (i) 70, (ii) 74, (iii) 78, and (iv) 82 for a crystal 10 unit cells thick and a beam direction along 00,10. Other conditions were appropriate to the microscope used.

a wider phase range in the higher temperature preparations and seemed to replace phases with wider *galena*-like slabs such as *L*7,7 or *L*8,8. Thus it is possible that the phases which contain even wider slabs of 9 or 11 octahedra are unstable at 773 K but would occur at lower temperatures of preparation.

The existence of a composition region where the twinned phases had a tendency

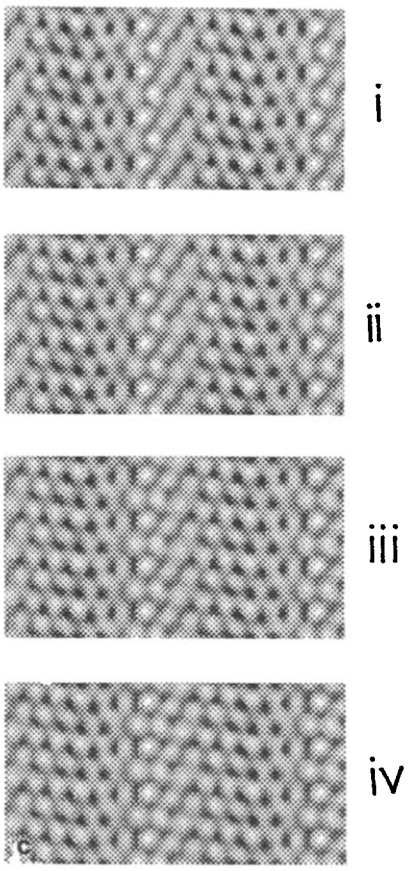

FIG. 4—*Continued*

to intergrow is also of interest. The intergrowths, mostly of *L*4,4 and *L*4,7, formed a continuum of structures instead of normally separated twinned phases. This result may throw some light on a disordered phase called *schimerite* reported by Makovicky and Karup-Møller (*11*). Schimerite has several characteristic features in common with the intergrowths found in this study. The most important of these is perhaps that the compositional field where schimerite was found extended from *L*4,4 through *L*4,7 to *L*7,7-rich areas, which is identical to the area of intergrowth in our studies. In addition, schimerite was reported to yield diffraction patterns displaying more or less diffuse structure reflections, rather than continuous streaking, and it was suggested that the structures represented a stacking of domains composed of sequences of *galena*-like slabs oriented parallel to each other. Similar diffraction effects can be seen on the electron diffraction pattern shown in Fig. 11b, for example, while the micrographs of the intergrowths directly reveal that the structures are composed of *galena*-like slabs oriented parallel to each other. This suggests that the intergrowths of *L*4,4 and *L*4,7 found in the present study are identical with mineral schimerite. An examination of mineral samples to test this hypothesis would be of interest.

At present it is difficult to be precise about why the addition of Ag_2S to the PbS–Bi_2S_3 system stabilizes the formation of slabs of *galena*-like structures eight octahedra and, to a lesser extent, five octahedra in width. However, calculations of elastic strain energy in lead bismuth sulfosalts of the type discussed here (*18*) have shown that the relative stability of the homologs in the *LN*,*N* series was critically dependent upon the distribution of the cations in the various sites available. As Ag has not only a different valence but also a different size to Pb, Bi, and S it is clear that its incorporation will lead to changes in the relative stability of the phases. As there is very little experimental data available on the distribution of Ag in these structures, recalculations of the elastic strain energy would seem premature.

It is clear from the studies reported here that considerable structural complexity exists in the Ag_2S–PbS–Bi_2S_3 system, and that only a part of it has been uncovered in this study. Further experiments, covering wider composition ranges and different preparation temperatures, are of considerable interest.

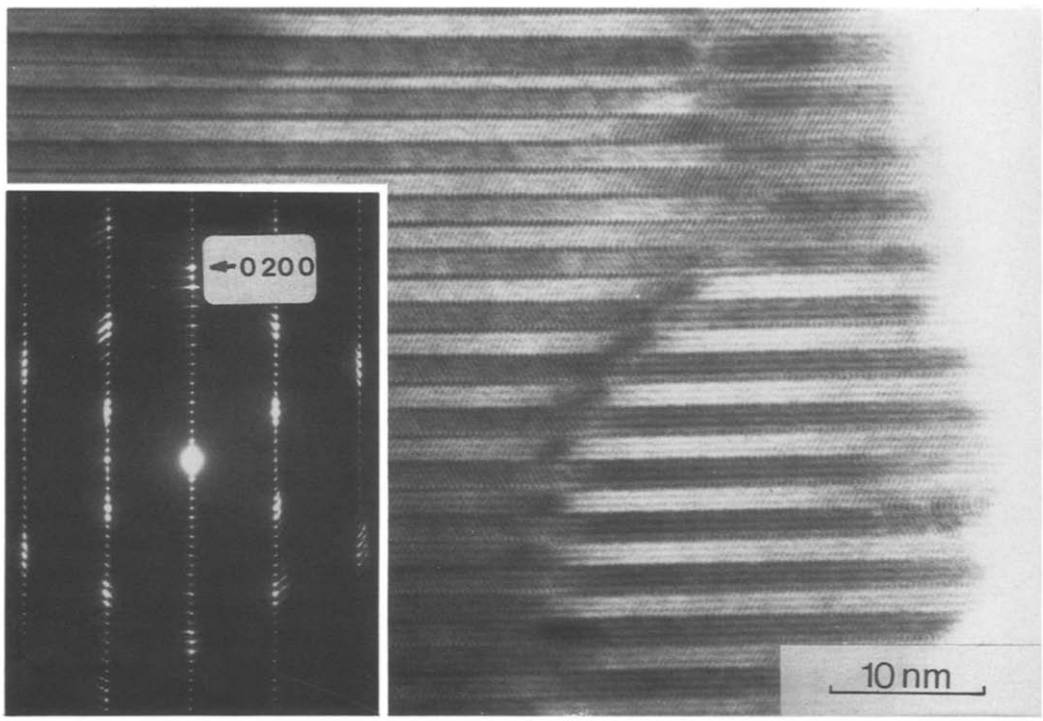

Fig. 5. Electron micrograph and inset the diffraction pattern of *L*8,8 close to the (001) projection. The 0,20,0 reflection on the diffraction pattern corresponds to the 311 reflection of the PbS subcell.

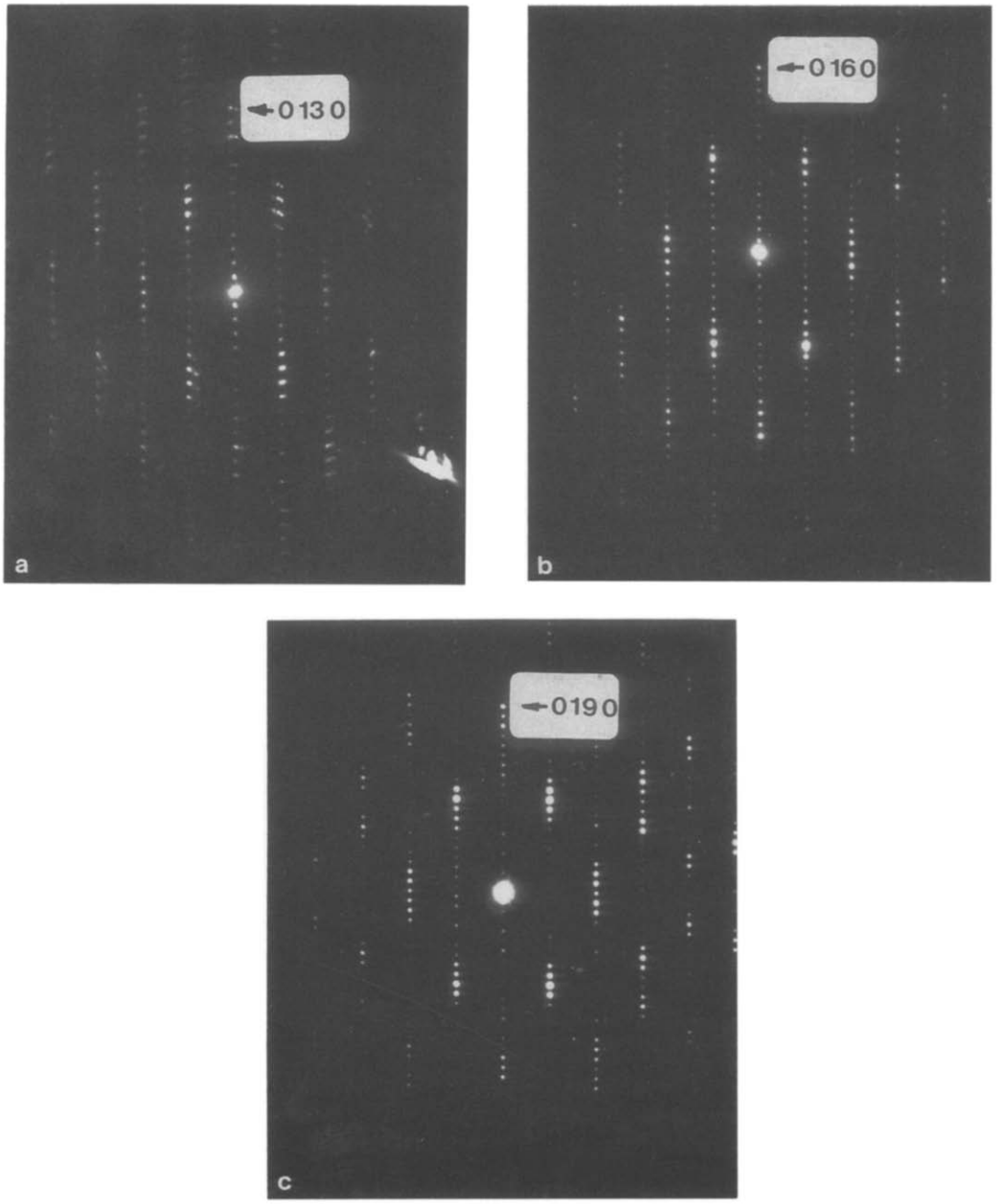

Fig. 6. Electron diffraction patterns of (a) *L*4,5, (b) *L*4,8, and (c) *L*7,8 taken with the electron beam parallel to (001). The reflections marked as 0,13,0 on (a), 0,16,0 on (b), and 0,19,0 on (c) correspond to the 311 reflection of the PbS subcell.

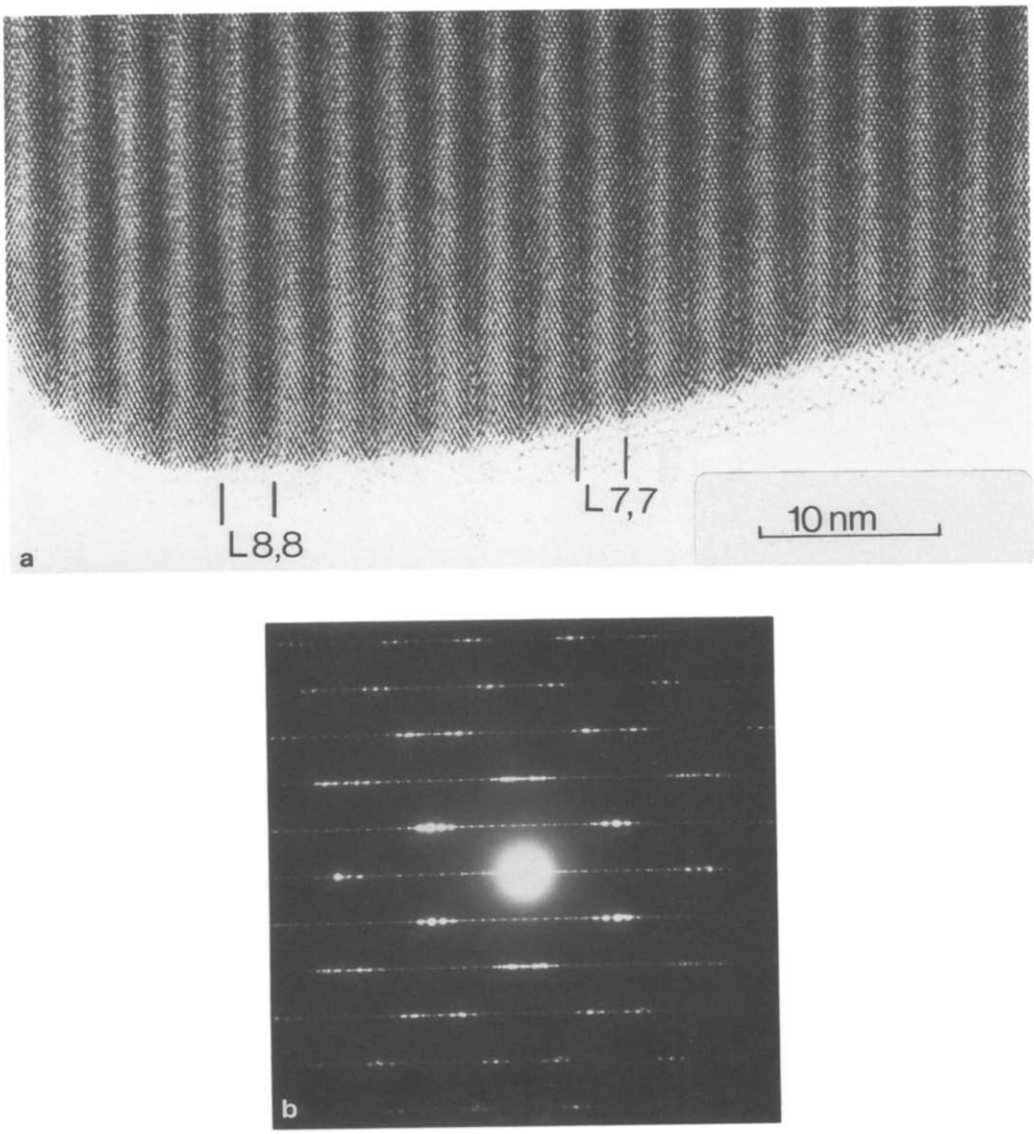

Fig. 7. (a) Electron micrograph of an intergrowth of $L7,7$ and $L8,8$. The twin planes are imaged alternatively in light and dark contrast. (b) Electron diffraction pattern of the crystal fragment shown in (a) revealing two sets of superimposed reflections corresponding to $L7,7$ and $L8,8$. The crystal fragment comes from a sample in the compositional region marked with a line on Fig. 2c.

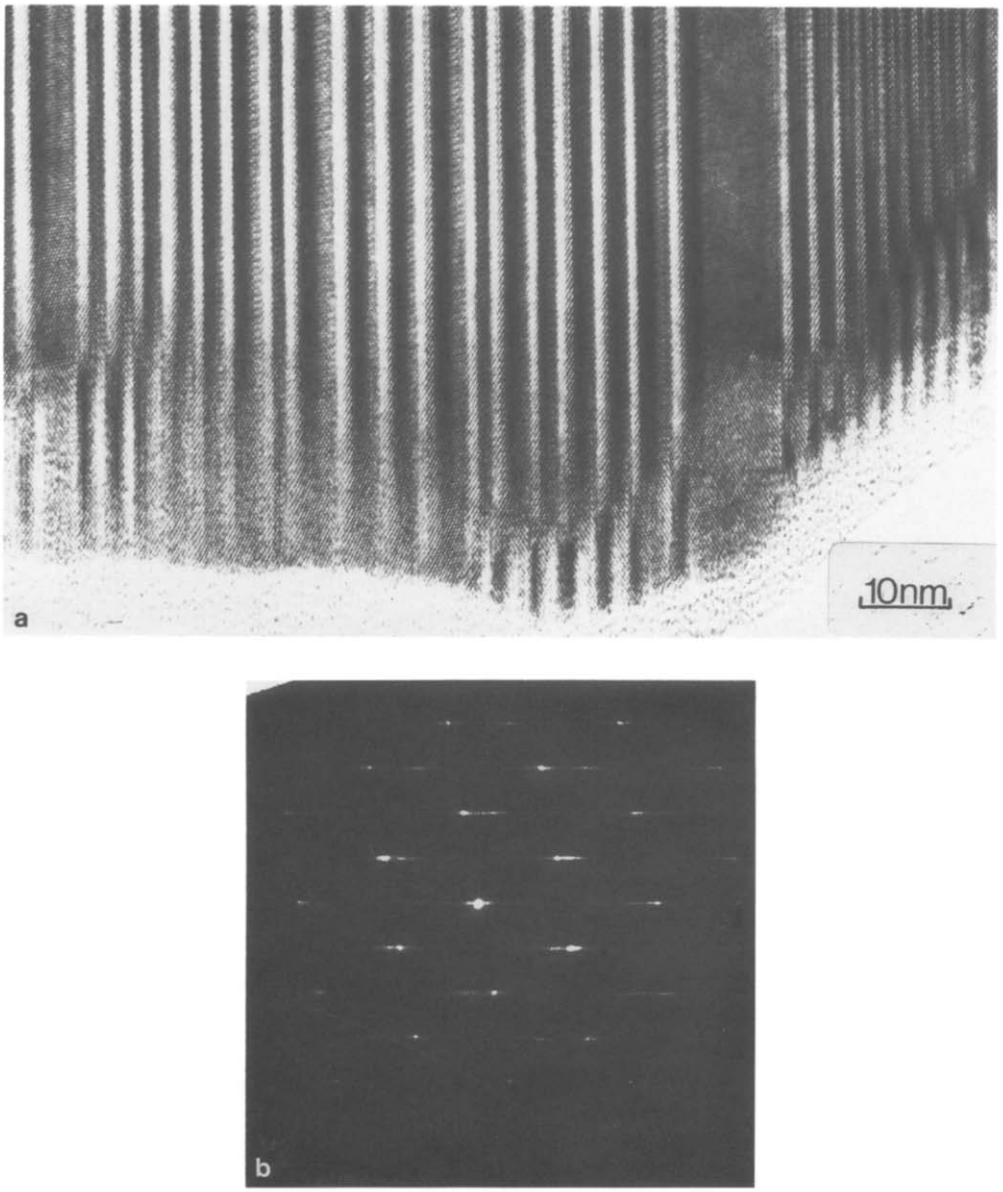

Fig. 8. (a) Electron micrograph and (b) electron diffraction pattern of a crystal fragment showing a disordered intergrowth of various widths of *galena*-like slabs. The diffraction pattern shows pronounced streaking.

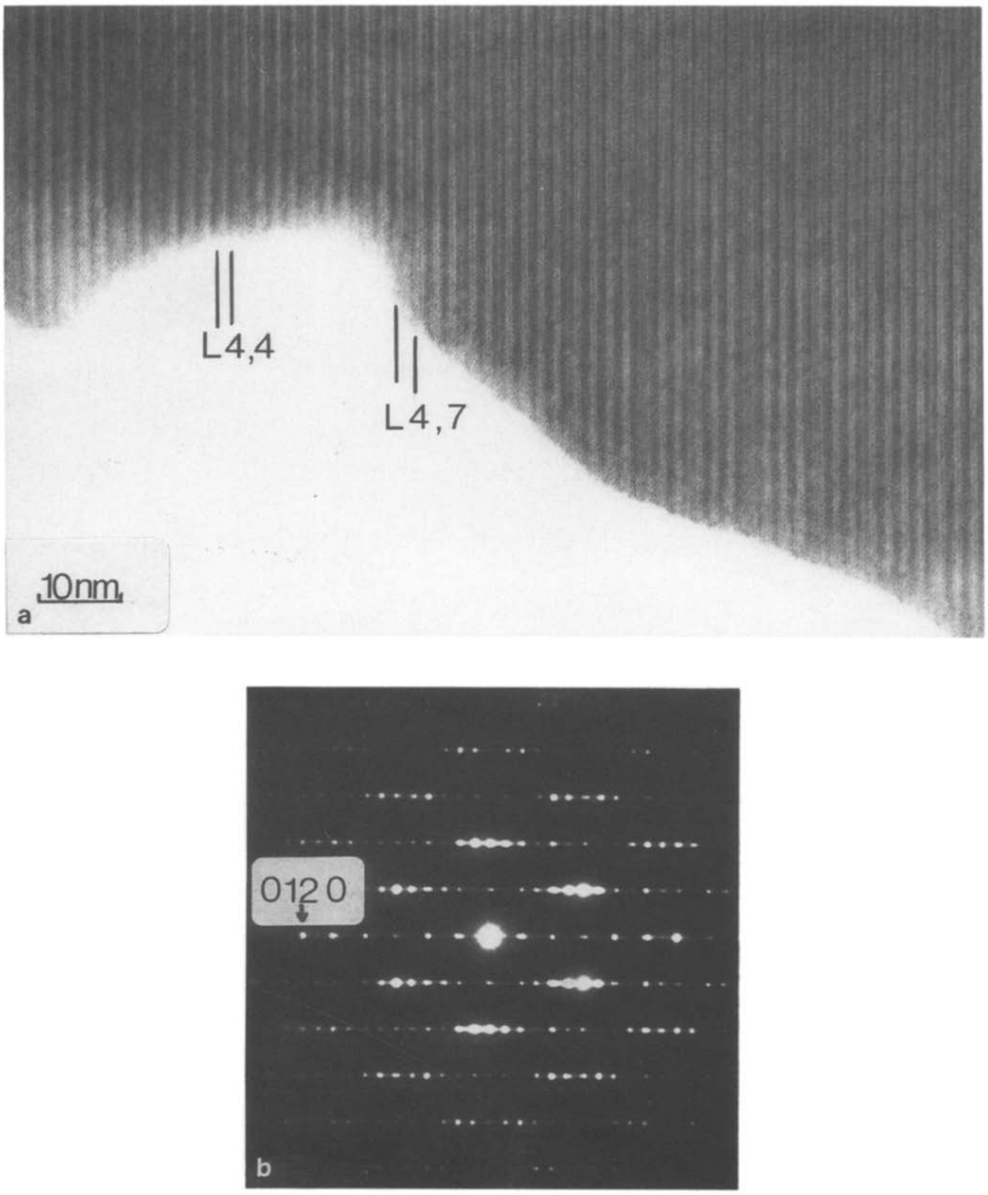

Fig. 9. (a) Electron micrograph and (b) electron diffraction pattern of a crystal fragment showing disordered intergrowth of $L4,4$ and $L7,7$. The rather sharp 0,12,0 reflection marked on (b), which corresponds to the 311 reflection of the PbS subcell, indicates that $L4,4$ is the predominant phase present in the crystal fragment.

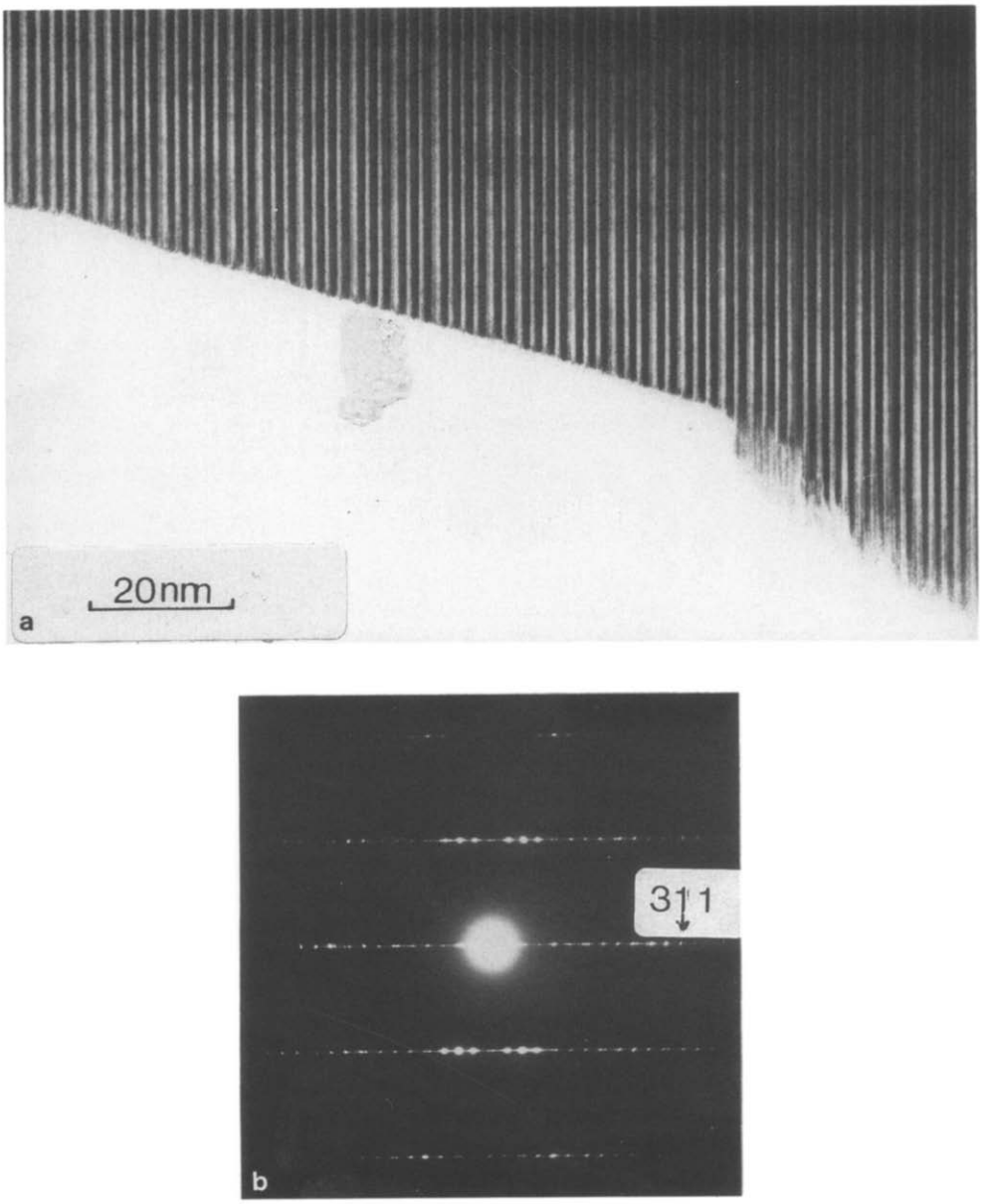

Fig. 10. (a) Electron micrograph and (b) electron diffraction pattern of a crystal fragment showing partial ordering of *galena*-like slabs. The spacing of the wider lattice fringes mostly corresponds to *galena*-like slabs seven octahedra in width and that of the narrower slabs to slabs four octahedra in width. Each of the sequences 7,4, 7,4,4, and 7,4,4,4 occur in this small region of crystal. The 311 PbS subcell reflection is marked on (b).

Acknowledgments

A.S. is indebted to the British Council and I.C.I plc. for financial support. Both authors are indebted to Neville Dodds for the computed images.

References

1. R. J. D. TILLEY, *in* "The Chemical Physics of Solids and their Surfaces" (M. W. Roberts and J. M. Thomas, Eds.), Chap. 6, The Royal Society of Chemistry, London (1980).
2. S. ANDERSSON AND B. G. HYDE, *J. Solid State Chem.* **9,** 92 (1974).
3. H. H. OTTO AND H. STRUNZ, *N. Jb. Mineral Abh.* **108,** 1 (1968).
4. Y. TAKÉUCHI AND J. TAKAGI, *Proc. Japan. Acad.* **50,** 76 (1974).
5. J. TAGAKI AND Y. TAKÉUCHI, *Acta Crystallogr. B* **28,** 649 (1972).
6. R. J. D. TILLEY AND A. C. WRIGHT, *Chem. Scr.* **19,** 18 (1982).
7. D. COLAÏTIS, D. VANDYCK, AND S. AMELINCKX, *Phys. Status Solidia* **68,** 419 (1981).
8. A. PRODAN, M. BAKKER, AND B. G. HYDE, *Phys. Chem. Miner.* **8,** 188 (1982).
9. S. KARUP-MØLLER, *Bull. Geol. Soc. Denmark* **26,** 41 (1977).
10. E. MAKOVICKY AND S. KARUP-Møller, *Neues Jahrb. Mineral. Abh.* **130,** 264 (1977).
11. E. MAKOVICKY AND S. KARUP-Møller, *Neues Jahrb. Mineral. Abh.* **131,** 56 (1977).
12. E. MAKOVICKY AND S. KARUP-Møller, *Neues Jahrb. Mineral. Abh.* **131,** 187 (1977).
13. D. VANDYKE, D. CALAÏTIS, AND S. AMELINCKX, *Phys. Status Solidia* **68,** 385 (1981).
14. J. SPENCE, "Experimental High Resolution Electron Microscopy," Oxford Univ. Press (Clarendon), London/New York (1981).
15. P. B. HIRSCH, A. HOWIE, R. B. NICHOLSON, D. W. PASHLEY, AND M. J. WHELAN, "Electron Microscopy of Thin Crystals," Butterworths, London (1965).
16. P. A. STADELMANN, *Ultramicroscopy* **21,** 131 (1987).
17. A. SKOWRON AND R. J. D. TILLEY, *J. Solid State Chem.* **78,** 84 (1989).
18. K. AIZAWA, E. IGUCHI, AND R. J. D. TILLEY, *J. Solid State Chem.* **48,** 284 (1983).